

Earth Rotation Parameters in Atmospheric Data Assimilation

Lisa Neef¹, Katja Matthes^{1,2}, Kevin Raeder³, Sebastian Wahl¹, and Nick Pedatella⁴

Corresponding author: L.J. Neef, Düsternbrooker Weg 20, D-24105 Kiel, Germany
(lneef@geomar.de)

¹Ocean Circulation and Climate
Dynamics - Marine Meteorology, GEOMAR
Helmholtz Centre for Ocean Research Kiel,
Kiel, Germany.

²Christian-Albrechts Universität zu Kiel,
Kiel, Germany.

³Institute for Mathematics Applied to
Geosciences, National Center for
Atmospheric Research, Boulder, Colorado,
USA.

⁴COSMIC Program Office, University
Corporation for Atmospheric Research,
Boulder, Colorado, USA.

Abstract. Variations in the atmosphere's angular momentum are observed consistently and at high accuracy in terms of variations in the Earth's rate of rotation and polar orientation. It has been suggested that these Earth rotation parameters could therefore be assimilated into atmosphere or ocean models in order to add extra information, either when conventional observations are sparse, or in addition. However, the atmospheric angular momentum represents global integrals of the wind and pressure fields, and it is unclear how a data assimilation system would distribute the information from such observations across model variable fields. To test this, we perform idealized assimilation experiments with the Community Atmosphere Model (CAM) within the Data Assimilation Research Testbed (DART), assimilating atmospheric angular momentum observations both in the presence and absence of local temperature observations. The experiments show that assimilating the atmospheric angular momentum suffers from a high sampling error relative to a very small state-to-observation covariances, and therefore generally leads to filter divergence. Nevertheless, comparing the experiments in terms of their angular momentum also illustrates the different constraints imposed in each case. This suggests that the Earth rotation parameters can be used as a tool to evaluate ensemble reliability and accuracy of a data assimilation system, without being assimilated. We illustrate this idea with a set of ensemble simulations of the Whole Atmosphere Community Climate Model (WACCM).

1. Introduction

Variations in the rotation and orientation of the Earth are measured regularly and at high accuracy using space geodesy [Gross, 1992; IERS, 2009]. These measurements contain information about the atmosphere, oceans, and continental hydrosphere, which all exchange angular momentum with the solid Earth, thereby causing both the Earth's rate of rotation and its polar orientation to fluctuate.

Because the atmosphere and ocean dominate sub-decadal Earth rotation variations, these observations are typically used to evaluate atmosphere simulations [Boer, 1990; Rosen and Salstein, 2000; Neef and Matthes, 2012], ocean simulations [Gross et al., 1996] or atmosphere reanalyses [Yu et al., 1999; Aoyama and Naito, 2000; Paek and Huang, 2012; Berrisford et al., 2011],

Saynisch et al. [2010, 2011] and *Saynisch and Thomas* [2012] took this idea a step further by assimilating the residual between observed Earth rotation parameters and the estimated atmospheric angular momentum –the residual being an estimate of the oceanic angular momentum– into two ocean models of varying complexity (along with standard oceanic observations such as temperature and salinity). Their simulations were able to close the Earth angular momentum budget by adjusting the modeled oceanic angular momentum, while simultaneously keeping the modeled ocean state in agreement with the other ocean observations. *Saynisch et al.* [2010] and *Saynisch and Thomas* [2012] showed that the axial angular momentum budget is mainly closed by changing large-scale model parameters such as the freshwater flux, while *Saynisch et al.* [2011] found that closing

the equatorial angular momentum budget in particular required changes in the model's current field.

These results suggest that an atmosphere model could also benefit from the assimilation of Earth rotation observation, especially since the atmosphere dominates subdecadal length-of-day variations and accounts for at least half of subdecadal polar motion variations. Many large-scale atmospheric phenomena that dominate local weather but are subject to longer-timescale climate fluctuations, such as the El Niño / Southern Oscillation [Fong Chao, 1984], sudden stratospheric warmings [Neef *et al.*, 2014] and the Madden Julian Oscillation [Weickmann *et al.*, 1992], all have discernible footprints in Earth rotation anomalies. Climate reanalyses, while heavily constrained by observations from the surface to the lower stratosphere, still have discrepancies in the atmosphere's angular momentum budget [Berrisford *et al.*, 2011; Lehmann and Nevir, 2012], and may therefore benefit from adding atmosphere angular momentum to the assimilated observations.

However, the studies of *Saynisch et al.* [2010, 2011] and *Saynisch and Thomas* [2012] also faced a major challenge in that they attempted to constrain large, global model fields with observations of three global parameters, which presents an underconstrained optimization problem. While these studies found that reconciling an ocean model to observed Earth rotation variations leads to physically plausible adjustments to the model fields, the solutions found by the data assimilation in these simulations may not have been unique or necessarily closer to the true state of the ocean.

This study examines the potential of observed Earth rotation variations to constrain an atmosphere model as an assimilated variable (Section 3), and as a tool to evaluate data assimilation systems (Section 4). Section 2 describes the data assimilation experi-

ments, observations assimilated, assimilation method, and models used. The results are summarized and discussed in Section 5.

2. Methods

This study employs experiments with the Data Assimilation Research Testbed [DART *Anderson et al.*, 2009], an open-source, community tool that provides ensemble-based data assimilation that is independent of a particular model and observation set. In the first set of experiments (Section 3), we use DART to assimilate idealized angular momentum observations into the Community Atmosphere Model (CAM). In the second set of experiments (Section 4), observations of Earth rotation parameters are used as proxies of the atmospheric angular momentum to evaluate a set of simulations assimilating real meteorological observations in the Whole Atmosphere Community Climate Model (WACCM). Interfaces have been developed between DART and both CAM [*Raeder et al.*, 2012, see Section 3] and WACCM [*Pedatella et al.*, 2013, see Section 4]. Section 2.1 describes DART and the assimilation method used. Section 2.2 then describes the observations, both idealized and realistic, that are assimilated, focusing in particular on observations Earth rotation parameters / angular momentum.

2.1. Data Assimilation System

Having advanced an ensemble of N model states to the time at which an observation is available, all ensemble filters unite two basic quantities: the observation y , and N prior estimates of the observation, y_n , predicted by the ensemble. Bayes' theorem states that the conditional probability distribution of the observation, given the prior ensemble estimate on the one hand, and the physical measurement on the other, is the product of

their probability distributions. The resulting joint (or posterior) probability distribution has variance

$$\sigma_{y,\text{po}}^2 = \left[\frac{1}{\sigma_y^2} + \frac{1}{\sigma_{y,\text{obs}}^2} \right]^{-1}, \quad (1)$$

where σ_y^2 is the prior variance of the observation implied by the ensemble, and $\sigma_{y,\text{obs}}^2$ is the variance of the observation itself (i.e. the measurement error). The ensemble mean of this joint probability distribution is given by

$$\langle y_n^{\text{po}} \rangle = \sigma_{y,\text{po}}^2 \left[\frac{\langle y_n \rangle}{\sigma_y^2} + \frac{y^{\text{obs}}}{\sigma_{y,\text{obs}}^2} \right]. \quad (2)$$

This means that the equivalent observations implied by each ensemble member must change by $\Delta y_n = y_n^{\text{po}} - y_n$, such that the new ensemble spread and mean satisfy (1) and (2), respectively. Given an update Δy_n in the observation space, the ensemble filter then computes a corresponding update in the model state (in this study: the wind, surface pressure, and temperature fields of an atmospheric model) via linear regression [Anderson, 2003]:

$$\Delta x_{i,n} = \left(\frac{c_{x_i y}}{\sigma_y^2} \right) \Delta y_n, \quad (3)$$

where $x_{i,n}$ represents a component of the model state for ensemble member n , and $c_{x_i y}$ represents the prior covariance between the state component x_i and the observation y .

Ensemble assimilation algorithms are novel because they estimate the covariance and variance terms in the above equations using an ensemble of model simulations, rather than prescribing them, i.e.

$$c_{x_i y} = \langle e_{x_i, n} e_{y, n} \rangle, \quad (4)$$

where

$$e_{x_i,n} = x_{i,n} - \langle x_{i,n} \rangle \quad (5)$$

$$e_{y,n} = y_n - \langle y_n \rangle \quad (6)$$

are the deviations of each ensemble member from the ensemble mean in the state space and observation space, respectively.

Thus the error statistics can vary in time and space (according to the physical relationships simulated in the model), and are updated with new information whenever a new observation comes in. In a successful ensemble assimilation system, these terms should reflect the true error statistics of the model system. If not, the ensemble filter will diverge, i.e. the uncertainty predicted by the ensemble will increasingly underestimate the true error, eventually leading to the rejection of new observations.

All experiments in this study use the Ensemble Adjustment Kalman Filter (EAKF) of *Anderson* [2001], which computes the linear regression (3) to compute the ensemble mean state space analysis, and then computes the state-space ensemble deviations that correspond to the updated ensemble variance (1) (see *Anderson* [2003] for details).

2.2. Atmospheric Angular Momentum Observations

Barnes et al. [1983] derived three equations that describe variations in the three components of atmosphere angular momentum:

$$\chi_1(t) = \frac{1}{\Omega (C_m - A_m) \left(1 - \frac{k_2}{k_s}\right)} [(1 + k_l) \Omega \Delta \mathbf{I}_{13}(t) + \Delta h_1(t)] \quad (7)$$

$$\chi_2(t) = \frac{1}{\Omega (C_m - A_m) \left(1 - \frac{k_2}{k_s}\right)} [(1 + k_l) \Omega \Delta \mathbf{I}_{23}(t) + \Delta h_2(t)] \quad (8)$$

$$\chi_3(t) = \frac{1}{\Omega C_m \left(1 + \frac{4k_2}{3k_s} \frac{C-A}{C}\right)} [(1 + k_l) \Omega \Delta \mathbf{I}_{33}(t) + \Delta h_3(t)]. \quad (9)$$

χ_1 and χ_2 represent the two vector components of angular momentum defined by the intersection of the equator with the 0° W and 90° meridians, respectively; χ_3 represents the axial component. The constants $k_2 = 0.295$, $k_s = 0.938$, and $k_l = -0.301$ represent the rotational, secular and load Love numbers, respectively, which quantify the rotational deformation of the Earth. $\Omega = 7.292115 \times 10^{-5}$ rad/s is the average rotation rate of the Earth. $C = 8.0365 \times 10^{37}$ kgm² and $A = 8.0101 \times 10^{37}$ kgm² represent the (3,3) and (1,1) components of the moment of inertia of the solid Earth, and $C_m = 7.1237 \times 10^{37}$ kgm² and $A_m = 7.0999 \times 10^{37}$ kgm² are the corresponding moments of inertia of the mantle and crust only (they are used in the above equations to decouple the core and mean mantle motion).

The \mathbf{I}_{ij} represent the components of the atmospheric inertia tensor:

$$I_{13} = - \int R^2 \cos \phi \sin \phi \cos \lambda dM \quad (10)$$

$$I_{23} = - \int R^2 \cos \phi \sin \phi \sin \lambda dM \quad (11)$$

$$I_{33} = \int R^2 \cos^2 \phi dM, \quad (12)$$

and the h_i the relative angular momentum (due to wind) in each direction:

$$h_1 = - \int R [u \sin \phi \cos \lambda - v \sin \lambda] dM \quad (13)$$

$$h_2 = - \int R [u \sin \phi \sin \lambda + v \cos \lambda] dM \quad (14)$$

$$h_3 = \int R u \cos \phi dM, \quad (15)$$

where $R = 6371.0$ km is the radius of the Earth.

Note that the axial terms [(12) and (15)] weight all longitudes equally in their integrals, which means that mass anomalies usually cancel in the global integral, such that the wind term, h_3 , dominates the axial angular momentum [Barnes *et al.*, 1983]. Nearly

the opposite is true for the equatorial angular momentum terms [(10)-(11) and (13)-(14)], which are larger if the variable fields are hemispherically asymmetric. For these functions, the mass terms (I_1 and I_2) are typically about an order of magnitude larger than the wind terms (h_1 and h_2) [Barnes *et al.*, 1983].

In reality, of course, we don't measure the atmospheric angular momentum but rather the variations in the Earth rotation parameters that the angular momentum variations excite, namely polar motion and anomalies in the length-of-day. The non-dimensional representation of the angular momentum in (7)-(9) makes it easy to map angular momentum changes to Earth rotation changes. Polar motion is measured in terms of two angles, p_1 and p_2 , that represent the location of the Earth's rotational axis in an inertial, celestial reference frame that is fixed in space and defined relative to a group of stars (the celestial ephemeris pole). Barnes *et al.* [1983] and later Gross [1992] showed that these vectors can be directly related to variations in the equatorial components of the Earth's angular momentum (χ_1 and χ_2) via a rotation into the inertial reference frame of the Chandler wobble (a free nutation of the Earth of frequency $\sigma_0 = 2\pi/433$ days, which results from the oblateness of the Earth's figure):

$$p_1 + \frac{\dot{p}_2}{\sigma_0} = \chi_1 \quad (16)$$

$$-p_2 + \frac{\dot{p}_1}{\sigma_0} = \chi_2, \quad (17)$$

where the overdots represent time derivatives.

Length-of-day anomalies are observed as $\Delta\text{LOD} \equiv \text{UT1} - \text{IAT}$, where UT1 denotes the universal time measured by geodetic instruments, and IAT is a reference time based on atomic clock measurements. Anomalies in the length-of-day correspond directly to

anomalies in the axial angular momentum:

$$\Delta \text{LOD} = \Delta \chi_3 \times \text{LOD}_0, \quad (18)$$

where LOD_0 denotes the nominal length-of-day (86400s).

3. Global Angular Momentum as an Assimilation Variable

3.1. DART-CAM Experiments

In this section we ask whether an atmosphere model could be constrained to the truth even more by assimilating these parameters into the Community Atmosphere Model [CAM *Neale et al.*, 2010]. CAM forms the atmospheric component of the NCAR Community Earth System Model (CESM). We have run CAM version 5.0 with a finite-volume dynamical core, $1.9^\circ \times 2.5^\circ$ horizontal resolution, and 30 hybrid-coordinate vertical levels, with a top near 2 hPa. The top three model levels (starting at about 14 hPa) constitute a “sponge” layer, where horizontal diffusion is applied to temperature, vorticity, and divergence in order to absorb vertically propagating planetary waves.

An 80-member initial ensemble of CAM states was generated by selecting the 1 Jan restart files from an 80-year CAM simulation, then running the entire ensemble forward for one year while assimilating 6-hourly temperature and wind observations. This roughly simulates reanalysis-type observations, and yields a tightly-constrained starting ensemble on 1 Jan 2009.

A reference CAM simulation, run from Jan - Feb 2009 with observed sea surface temperatures as a boundary condition, constitutes the “truth” from which we generate a set of synthetic observations for assimilation. From this truth, we generate synthetic observations of χ_1 , χ_2 , and χ_3 every 24 hours, reflecting the observation frequency of the real

Earth rotation data series published by the International Earth Rotation Services [*IERS*, 2009], as well as the temperature observations on a uniform, global grid (amounting to roughly 2700 observations per day). The angular momentum observations are generated with zero observation error, to minimize sampling error effects and simulate an ideal situation where the Earth rotation parameters perfectly capture the atmospheric angular momentum. Separate experiments testing various values of observation error did not significantly change the results described below.

Four DART-CAM experiments are performed, summarized in Table 1. Each experiment integrates the 80-member CAM ensemble forward over 2009. The first experiment is a reference ensemble with no assimilation. Three following experiments assimilate synthetic observations, first of the angular momentum alone, then temperature observations alone, and finally local temperature observations along with the angular momentum. The latter two experiments only ran for 31 and 17 days, respectively, because this amount of integration time was found to be sufficient to compare the relative error reduction in the two experiments (see Fig. 1).

This analysis is similar to the studies of *Saynisch et al.* [2010, 2011] and *Saynisch and Thomas* [2012], with two main differences: (1) We use an atmosphere rather than an ocean model. (2) We assimilate synthetic observations generated from a model simulation that serves as the “true state”. This allows us to measure the true error, and also simulates an idealized situation where the atmosphere accounts for 100% of Earth rotation variations, which means that our experiments do not require an estimate of the oceanic or hydrospheric contributions to Earth rotation variations.

3.2. Observation-space diagnosis

Figure 1 compares the angular momentum components χ_2 and χ_3 for the three DART-CAM ensembles, their means, and the synthetic observations. The ensemble fits to χ_1 look qualitatively similar to χ_2 for all experiments and have been omitted for simplicity.

With no assimilation (“No DA”, first column), the angular momentum functions again show how the ensemble spreads about the truth, and how the spread saturates after about one month. If we assimilate the angular momentum functions alone (“AAM DA”, second column), the ensemble predictably clusters close to the true angular momentum, and captures the day-to-day angular momentum variations. The difference between the first two columns indicates that assimilating the angular momentum has imposed some constraint upon the wind, temperature, and surface pressure fields, though, as will be shown below, this does not necessarily mean that those fields have also moved closer to the true state.

The ensemble clusters even more tightly around the truth when instead of the angular momentum functions we assimilate local temperature observations (“Temp DA”, third column), which is a much stronger constraint on the model fields. Finally, adding the angular momentum observations to the regularly-spaced temperature observations (“Temp + AAM DA”, fourth column) slightly increases the agreement between the ensemble and the true state further. This suggests that the angular momentum observations may contain additional information that complements the information in the temperature observations, but it does not tell us whether the actual model fields have been improved, and if so, how. The next section will therefore examine how the update seen in the observation space translates into an increment in the state space.

3.3. State Update from Angular Momentum Observations

When an angular momentum observation is assimilated, the filter updates the state variables (i.e. the wind, temperature, or surface pressure at some point) according to the covariance between each state component and the global angular momentum component in question (χ_1, χ_2 , or χ_3) (3). One could simply estimate these covariances using a function proportional to the geographic weighting terms in each integral (e.g. the $\cos^2 \phi$ term in (12)), or some sort of mean covariance for a given timescale, as in *Nastula et al.* [2009]. The ensemble filter, however, computes these covariances from the ensemble using (4).

Using the ensemble to compute the covariances means that the physical relationship between local variable fields and the global angular momentum, as well as the variance of the model variables themselves, enter the covariance estimate statistically. If we abbreviate the angular momentum integrals [(10)-(15)] as

$$y_j = \sum_{i=1}^M f_{i,j} x_i, \quad (19)$$

where $f_{i,j}$ represents the spatial weighting that is applied to state component i for angular momentum component j , times the latitude, longitude, and mass increments in the integrals, and M represents the number of variables in the model state, the observation error terms in (4) become

$$e_{y_{j,n}} = y_{j,n} - \langle y_{j,n} \rangle = \sum_{k=1}^M f_{k,j} e_{x_k,n}, \quad (20)$$

which means that the state-to-observation covariance term becomes

$$c_{x_i y_j} = \frac{1}{N-1} \sum_{n=1}^N \left[e_{x_i,n} \sum_{k=1}^M f_{k,j} e_{x_k,n} \right]. \quad (21)$$

Thus for a given point x_i in the model state, the covariance to angular momentum component y_j is proportional to the ensemble spread at that point ($\frac{1}{N-1} \left[\sum_{n=1}^N e_{x_i,n}^2 \right]$) times the weighting function at that point ($f_{i,j}$), plus the sum of the covariances between

x_i and all other other points in the model state $[\frac{1}{N-1} \sum_{n=1}^N e_{x_{i,n}} e_{x_{k,n}}]$, each multiplied by their respective weighting functions ($f_{k,j}$). This makes physical sense: a point will be updated by an angular momentum observation if it is located in a region that is weighted strongly for that particular angular momentum component, and/or if it happens to covary strongly with other points that are strongly weighted in the integrals.

Figure 2 shows snapshots of the covariance between the zonal wind field and χ_3 (over the Northern Hemisphere, and the simulation assimilating only the angular momentum), on a tropospheric level [320 hPa; (a), (c), and (e)], and on a stratospheric level [10 hPa; (b), (d), and (f)]. The top row shows covariances on 20 Jan, the second ten days later on 30 Jan, and the bottom row shows covariances averaged over the time period 15 Jan - 28 Feb (right column). Figure 2 gives two reasons why the four-dimensional covariances estimated by the ensemble filter should be advantageous over static covariances. First, the covariance pattern for neither region or date resembles the weighting function of the axial wind integral (15), which means that the individual variances of the model variables, and the covariances between model variables, matter. The covariances estimated by the filter in the stratosphere [Fig. 2(b),(d), and (f)] also have much larger scales, reflecting the larger-scale dynamics of this region. Second, comparing the covariances at different points in time, and their much weaker time-average signal [(e) and (f)] shows that the covariances themselves vary strongly in time, which tells us again that a four-dimensional covariance model is necessary.

However, the covariances in both regions on the order of $10^{-12} \text{m}^2/\text{s}^2$. Even though the stratospheric contribution to the angular momentum is much smaller than that of the troposphere [Rosen and Salstein, 1985; Zhou et al., 2008], the magnitudes of the co-

variances are similar in the stratosphere and the troposphere, because the winds have higher variance in the stratosphere.) Considering the standard deviation of the zonal wind (of order 10 m/s) and the (dimensionless) axial angular momentum (of order 10^{-9}), the corresponding state-to-observation correlations turn out to be on the order of 10^{-4} . The minuscule correlations are not surprising, given that each individual state component contributes only a small amount to the global angular momentum integral, but to correctly estimate them, the correlations need to be significantly larger than the sampling error that comes from using a finite ensemble, which scales as $1/\sqrt{N}$ [*Houtekamer and Mitchell, 1998*]. This means that we would need upwards of $N = 1000$ ensemble members to compute correlations that have at least the same order of magnitude as their sampling error, which is not computationally feasible. To see whether the ensemble filter's dynamical covariance estimate can outweigh the effects of sampling error, we must look at the error in the idealized assimilation experiments.

Figure 3(a)-(b) shows the prior true error (true state minus posterior ensemble mean) at assimilation time on 30 Jan for 320 hPa (a) and 10 hPa (b). Ideally, the true error should look similar to the analysis increment (ensemble mean posterior - ensemble mean prior) (Fig. 3(c)-(d)). It is not surprising that the increments are an order of magnitude smaller than the true error since a single angular momentum observation has to be spread over the entire state, but in many regions, such as the stratospheric eastern hemisphere, the increment does not even go in the same direction of the true error, i.e. the adjustment following the insertion of the angular momentum moves the state even farther from the truth.

Therefore, to see whether the assimilation increment on 30 Jan has improved things or not, we check the increment in the mean square error on the same day (Fig. 3(e)-(f); here red shading means that the assimilation has reduced the distance between the ensemble mean and the truth). Clearly, the assimilation has successfully reduced the zonal wind error in some regions, but increased it by roughly the same amount elsewhere.

A successful ensemble data assimilation system must not only reduce error, but also reflect the correct error statistics in the updated ensemble. This means that the ensemble spread should be large enough that the true state can be considered a sample of the probability distribution represented by the ensemble, in which case

$$E_i = \frac{N+1}{N} S_i, \quad (22)$$

where S_i is the ensemble spread in some state variable and $E_i = (\langle x_i \rangle - x_i^t)^2$ is the RMS error in that variable [Huntley and Hakim, 2009; Murphy, 1988]. Figure 3(g)-(h) shows the increment (posterior minus prior) in the scaled ensemble spread (the right hand side of (22)). Assimilating the angular momentum decreases error only in some regions [Fig 3(e)-(f)], but it decreases the ensemble spread everywhere, following (2) -(3). The assimilation of angular momentum has therefore created a divergent data assimilation system, where the ensemble will increasingly cluster around a mean state that is farther from the truth than implied by the ensemble.

To illustrate this result on a local level, Figure 4 compares the zonal wind in the ensemble and its mean to the true state, for no assimilation (left column) and assimilating the angular momentum (right column). The ensemble in each cases is shown as averages over two regions: the tropospheric jet over the Atlantic (averaging between 30N-40N, 280W-360W, and 300hPa-200hPa), and the northern stratospheric polar vortex (averag-

ing between 60N-90N, 30-24 hPa, and all longitudes). For both measures, the angular momentum assimilation over the first two weeks clearly decreases the ensemble's spread about the mean, and gives the ensemble mean more realistic variations (which average out in the ensemble with no assimilation). However, only the polar vortex winds, which showed a more large-scale covariance structure (Fig. 2) show slight improvement relative to the truth, and only for the first few weeks of assimilation.

That we see some improvement in the state estimate when assimilating the global angular momentum is a remarkable result given the high sampling error in the state-to-observation covariances. This improvement is nevertheless small, limited to regions with large-scale correlation patterns, and fades as the assimilation progresses and the ensemble spread increases. A natural next question is to ask whether angular momentum observations could improve the state more if the ensemble spread is kept small by the assimilation of other, spatially localized, observations. This question will be treated in the next section.

3.4. Assimilating AAM in the Presence of Conventional Observations

Even when a given observation is unable to significantly constrain a modeled state by itself, it may still improve the assimilation of other, more conventional observations. Figure 1 column 3 shows that assimilating temperature observations alone into the ensemble is sufficient to achieve a good fit to the true angular momentum. But then adding observations of the angular momentum improves the fit further, which implies that the angular momentum observations add information to the ensemble. If we assimilate angular momentum (or Earth rotation) observations along with local observations that bring the ensemble mean closer to the true state, the angular momentum observations could

perhaps push the ensemble even closer to the truth by adding the additional requirement that the modeled angular momentum should match observations. But whether or not the small and error-frought state-to-observation covariances of the angular momentum really add value to the state estimate is not obvious, and here again we examine the true error in idealized experiments with 80-member CAM ensembles.

Figure 5a shows the increment (posterior-prior) in the global-average ensemble variance in the zonal wind, assimilating global temperatures with and without additional angular momentum observations. The increment in the ensemble spread is always negative [following (1)], and adjusts from an initially weak value to a stronger steady-state value as the ensemble, which was initially constrained by both wind and temperature observations, adjusts to being constrained only by temperature observations. During this early period, adding the angular momentum observations causes a slightly stronger adjustment of the ensemble variance, indicating that the angular momentum observations add some information to the state estimate. However, comparing the posterior-prior difference in the mean square error of the ensemble mean (Fig. 5b) shows that adding the angular momentum observations actually results in a weaker error reduction during the adjustment period (1-5 Jan). Although the additional angular momentum observations do not add any additional certainty (Fig. 5a) once the ensemble variance has reached steady state (after about 9 Jan), the absolute posterior mean square error (Figure 5c) is consistently larger when the angular momentum observations are added. Thus the additional observations increase the global mean error at worst (at the beginning of the assimilation), and have no impact at best (at steady-state). We therefore find no clear benefit of assimilating

atmospheric angular momentum (or Earth rotation parameter) observations, either with or without the assimilation of conventional observations.

4. Global Angular Momentum as an Evaluation Variable

Having found that it is extremely difficult to assimilate the atmospheric angular momentum effectively, we now ask whether Earth rotation variables may be useful as an independent variable for evaluation of data assimilation systems, because it is difficult, in practice, to judge whether data assimilation has actually brought a model closer to the truth, since the truth isn't known and independent observations that cover the same temporal and spatial domain as the assimilated observations often don't exist. The three atmospheric angular momentum components are sometimes used to evaluate reanalysis data [*Yu et al.*, 1999; *Aoyama and Naito*, 2000; *Paek and Huang*, 2012; *Berrisford et al.*, 2011] because they are easy to compute from the modeled wind and pressure fields, freely available at daily resolution, updated continuously, and available since the 1960s (and at high accuracy since about 1980).

The ensemble filter gives us an ensemble of atmospheric angular momenta and therefore information not just about the estimated model state but also its uncertainty. In this section we show how this works by taking advantage of a set of three recent DART-WACCM ensemble simulations of the winter 2009/10, assimilating meteorological observations.

4.1. DART-WACCM Experiments

WACCM extends the dynamical core of CAM up to 5×10^{-6} hPa (circa 140 km, in the lower thermosphere) with 66 levels, and includes additional chemical and physical processes for these regions. The experiments here use WACCM version 4 with full interactive

chemistry. WACCM's three highest model levels (starting from about 2×10^{-5} hPa) have strong horizontal diffusion to absorb planetary waves. The DART-WACCM simulations shown here, like the CAM experiments in the previous section, have $1.9^\circ \times 2.5^\circ$ horizontal resolution.

Three DART-WACCM experiments are examined (Table 1); each runs a 40-member WACCM ensemble from 1 Oct 2009 to 31 Jan 2010. The first experiment is simply a WACCM ensemble with no assimilation, while the second assimilates the meteorological observations that are used in the NCEP/NCAR reanalysis, i.e. winds and temperatures from radiosondes and aircraft [Saha *et al.*, 2010], as well as refractivity profiles measured via GPS radio-occultation by the COSMIC satellite constellation [Anthes *et al.*, 2008]. The observations extend from the surface to about 2 hPa. A third experiment assimilates the same observations, but only in the tropical band (30S - 30N).

In the cases with assimilation, the impact of the observations is localized using a Gaspari-Cohn function [Gaspari and Cohn, 1999] with a half-width of 0.2 radians in the horizontal, and 0.5 scale heights in the vertical. Adaptive ensemble inflation [Anderson, 2009] increases the ensemble spread when too many observations are rejected; the inflation factor varies in space and time and is proportional to the distance between the ensemble mean and the observation, given the uncertainties of each. No analysis increment is allowed above 0.1 hPa, in order to prevent the generation of spurious gravity waves resulting from a large ensemble spread due to the sparsity of upper level observations [Polavarapu *et al.*, 2005].

4.2. Using AAM to evaluate DART-WACCM Assimilation Runs

The three DART-WACCM simulations (Table 1) represent three ensembles with varying levels of observational constraint. To evaluate the strength of the constraint in each case, we might compare their respective ensemble variances. For example, the global mean ensemble variance of the zonal wind (Fig. 6) is lowest for global assimilation and highest for no assimilation, while assimilating in the tropics only gives an ensemble variance somewhere in between. This tells us (to no surprise) that assimilating fewer observations results in a less certain simulation, but it does not tell us anything about the relative accuracy of the three ensembles, nor to what extent the ensembles might be diverging from the truth. A local peak in ensemble variance of the global assimilation case on 17 Dec (A) suggests that the adaptive inflation algorithm has detected some divergence of the ensemble from the observations, causing the filter to artificially increase the ensemble spread. We could check whether more observations are rejected around this time, but that still does not tell us much about the reliability of the ensemble, i.e. whether observations were rightfully rejected or not. Moreover it is unclear why the ensemble variance grows much more quickly in the two assimilation cases relative to the no-assimilation case, in the first week of assimilation (B). A comparison to independent (non-assimilated) observations is therefore needed.

Geodetic monitoring of the polar motion and length-of-day anomalies supplies us with 24-hourly observations of the global angular momentum. Of course, the Earth rotation parameters also reflect the angular momenta of the oceans, the continental hydrosphere, and solid Earth, but on subseasonal to interannual timescales, χ_2 and χ_3 are dominated by the atmosphere's angular momentum. (Subseasonal variations in χ_1 have a stronger

oceanic contribution because the longitudinal terms in the χ_1 integrals [(10) and (13)] weight mass and zonal wind anomalies more strongly over the oceans, whereas the χ_2 integrals weight them more strongly over the continents; e.g., *Neef and Matthes* [2012].) Of these, χ_3 suffers from the undefined constant of integration in the relationship between observed length-of-day anomalies and the atmospheric angular momentum, which means that we can really only compare the variations in modeled and observed χ_3 , but not the absolute values.

We therefore focus here on the equatorial component χ_2 , which is a function of the two components of the polar motion [see(17)] as an independent/evaluation variable. Comparing χ_2 for each of the WACCM ensembles (Fig. 7) to the corresponding value implied by polar motion observations [using (17)] shows not only the relative ensemble spread between the three cases (which we also see in Fig. 6), but also the relative accuracies of the ensemble mean in each case. For example, we can see that assimilating only in the tropics actually results in a fairly accurate ensemble mean, despite the larger ensemble variance. We can also see that the anomalously large ensemble variance on 17 Dec in the global-assimilation case (A) does indeed follow a period of filter divergence, where the ensemble variance is persistently smaller than the distance to observations. The greater ensemble spread seen at the start of the assimilation period for the global-DA and tropical-DA cases (B) can also be explained by examining χ_2 , because this variable shows how adding the first observation at the initial time immediately corrects a strong bias in the model fields, which then increases the ensemble spread.

Figure 7 echoes the assertion of *Yamaguchi et al.* [2015], who showed that comparing the spread of an ensemble in observation space to its square-error relative to observations,

is a more accurate measure of ensemble reliability than comparing an ensemble against a meteorological analysis. The Earth rotation parameters are good candidates for such an observation-based ensemble verification because they are independent observations and simple to compute, and easily demonstrate how the over- or underdispersiveness of the ensemble evolves in time. The projection of polar motion onto angular momentum component χ_2 is the most useful parameter for a stand-alone atmosphere simulation, but for coupled or Earth-system simulations, χ_1 would be similarly useful, while χ_3 can be used to evaluate long-term anomalies.

5. Summary and Discussion

We have evaluated the potential for using observations of Earth rotation parameters to evaluate data assimilation systems and constrain atmospheric models as assimilated variables. Because they are freely available at high accuracy and relatively high temporal resolution and updated continuously [IERS, 2009], Earth rotation parameters are useful as simple observables against which to validate the constraint imposed by observations in a data assimilation system. Comparing the angular momentum of a model ensemble to these observations is computationally straightforward; for a standalone atmosphere model, component χ_2 is the most useful because it is the most dominated by the atmosphere and can be easily related to polar motion without an ambiguous constant of integration. This comparison gives a global view both of how well the modeled wind and mass fields approximate the truth. The Earth rotation parameters have been connected to various atmospheric models, and their oceanic residuals have even been used to constrain an ocean model via data assimilation [Saynisch et al., 2010, 2011; Saynisch and Thomas, 2012].

However, assimilation experiments with synthetic observations and a known truth showed that it is difficult to constrain the model state with angular momentum observations because they are global integrals of the model fields, which leads to associated state-to-observation covariances that are much smaller than any realizable ensemble sampling error (Fig. 2). Thus the ensemble filter used in this study generates a covariance model that is physically plausible and computes the statistically most likely update of each state space component, but because of sampling error it is common that the state update computed by the filter moves the ensemble and its mean farther away from the true state, while still satisfying the angular momentum observations (red contours in Fig. 3). Though the global angular momentum observations can impose a weak constraint on some aspects of the modeled state (Fig. 4), it is not enough to yield a reliable and robust correction to the model state.

One might therefore expect that global angular momentum observations can constrain the modeled state better if the ensemble is already largely constrained to the truth by more conventional, spatially-localized observations. We tested this idea by assimilating a global grid of synthetic temperature observations in addition to the global angular momentum observations. We found that, overall, adding the angular momentum observations worsens the analysis (Fig. 5c), because the sampling error inherent in the angular momentum assimilation inhibits error reduction in the analysis increment.

A common technique for avoiding divergence of an ensemble filter is to periodically inflate the ensemble about its mean. It is unlikely that ensemble inflation would help here, since we found that the filter diverges both when the ensemble spread is large (section

3.3) and when it is very small (section 3.4). We have seen in a set of short assimilation runs with ensemble inflation (omitted here for brevity), that this is indeed the case.

Even though this study focused on an atmosphere model, the results can likely be extended to ocean models, where the state vector, although smaller, is still many orders of magnitude larger than the observation vector, and this would also yield state-to-observation correlations that are much smaller than the sampling error. For the ocean, it is possible to adjust the freshwater flux into the model, rather than the prognostic state variables, as a control parameter (as in *Saynisch et al.* [2010] and *Saynisch and Thomas* [2012]), but this has no corollary in atmosphere models.

Overall, this work illustrates the difficulties of assimilating observations that represent integrals or averages of the model state. *Dirren and Hakim* [2005] proposed a variation of the ensemble filter to deal with observations that are temporal averages of the state; their alternative algorithm projects the observation increment only on the time-average of each ensemble member while keeping deviations from the average untouched. *Huntley and Hakim* [2009] showed that applying this method in a global atmosphere model reduces errors over a wide range of scales, and that one can even improve instantaneous errors when only time-average observations are assimilated. It is conceivable that this approach could be extended to the assimilation of Earth rotation parameters, by updating the global-average contribution to the angular momentum at each gridpoint, and thereby improve the state estimate. However, for assimilation systems on the scale of DART-CAM and DART-WACCM, this would require major changes in the code structure, while the possible gains of such a step are not clear.

Another alternative pathway may be to assimilate the rate-of-change of Earth rotation parameters, thereby constraining the total torque between the atmosphere and the solid Earth. The net torque is the sum of pressure gradients over topography (the so-called mountain torque), surface friction, and torque due to topographic gravity waves [Lejen  s *et al.*, 1997]. Appropriate control variables could be the surface pressure, orographic gravity wave drag parameters, or surface friction. We defer exploration of this idea to future research.

Acknowledgments. The computations discussed in this study were performed at the Deutsches KlimaRechenZentrum (DKRZ) in Hamburg, Germany. We are grateful to Nancy Collins and Christopher Kadow for help with porting DART to the DKRZ supercomputer. This work has been performed within the Helmholtz-University Young Investigators Group NATHAN, funded by the Helmholtz-Association through the President's Initiative and Networking Fund, the GEOMAR Helmholtz Centre for Ocean Sciences Kiel, the Helmholtz Centre Potsdam GFZ German Research Centre for Geosciences, and Freie Universit  t Berlin.

References

- Anderson, J., T. Hoar, K. Raeder, H. Lui, N. Collins, R. Torn, and A. Avellano (2009), The data assimilation research testbed: A community facility, *Bull. Am. Met. Soc.*, pp. 1283–1296, doi:10.1175/2009BAMS2816.1.
- Anderson, J. L. (2001), An ensemble adjustment filter for data assimilation, *Mon. Wea. Rev.*, 129, 2884–2903.

Anderson, J. L. (2003), A Local Least Squares Framework for Ensemble Filtering, *Mon. Weather Rev.*, 131(4), 634–642, doi:10.1175/1520-0493(2003)131<0634:ALLSFF>2.0.CO;2.

Anderson, J. L. (2009), Spatially and temporally varying adaptive covariance inflation for ensemble filters, *Tellus A*, 61(1), 72–83, doi:10.1111/j.1600-0870.2008.00361.x.

Anthes, R. A., et al. (2008), The COSMIC/FORMOSAT-3 mission: Early results, *Bull. Am. Met. Soc.*, 89(3), 313–333, doi:10.1175/BAMS-89-3-313.

Aoyama, Y., and I. Naito (2000), Wind contributions to the earth's angular momentum budgets in seasonal variation, *J. Geophys. Res.*, 105, 12,417–12,431.

Barnes, R., R. Hide, F.R.S., A. White, and C. Wilson (1983), Atmospheric angular momentum fluctuations, length-of-day changes and polar motion, *Proc. Roy. Soc. London*, 387, 31–73.

Berrisford, P., P. Källberg, S. Kobayashi, D. Dee, S. Uppala, A. J. Simmons, P. Poli, and H. Sato (2011), Atmospheric conservation properties in ERA-Interim, *Quart. J. Roy. Meteorol. Soc.*, 137(659), 1381–1399, doi:10.1002/qj.864.

Boer, G. (1990), Earth-atmosphere exchange of angular momentum simulated in a general circulation model and implications for the length of day, *J. Geophys. Res.*, 95, 5511–5531.

Dirren, S., and G. J. Hakim (2005), Toward the assimilation of time-averaged observations, *Geophys. Res. Lett.*, 32(4), L04,804, doi:10.1029/2004GL021444.

Fong Chao, B. (1984), Interannual length-of-day variation with relation to the southern oscillation/El Niño, *Geophys. Res. Lett.*, 11(5), 541–544, doi:10.1029/GL011i005p00541.

- Gaspari, G., and S. E. Cohn (1999), Construction of correlation functions in two and three dimensions, *Quart. J. Roy. Meteorol. Soc.*, 125, 723–757, doi:10.1002/qj.49712555417.
- Gross, R. S. (1992), Correspondence between theory and observations of polar motion, *Geophys. J. Int.*, 109, 162–170.
- Gross, R. S., K. H. Hamdan, and D. H. Boggs (1996), Evidence for excitation of polar motion by fortnightly ocean tides, *Geophys. Res. Lett.*, 23(14), 1809–1812.
- Houtekamer, P., and H. L. Mitchell (1998), Data Assimilation Using an Ensemble Kalman Filter Technique, *Mon. Weather Rev.*, 126(1969), 796–811.
- Huntley, H. S., and G. J. Hakim (2009), Assimilation of time-averaged observations in a quasi-geostrophic atmospheric jet model, *Clim. Dyn.*, 35(6), 995–1009, doi:10.1007/s00382-009-0714-5.
- IERS (2009), *IERS Earth Orientation Data*, IERS: Int. Earth Rot. and Ref. Service, Bundesamt für Kartographie und Geodäsie (BKG), Frankfurt am Main, Germany, available online at <http://www.iers.org>.
- Lehmann, E., and P. Nevir (2012), Uncertainties in relative angular momentum computed from zonal winds in reanalysis data, *J. Geophys. Res.*, 117, D09,101.
- Lejenäs, H., R. R. Madden, and J. J. Hack (1997), Global atmospheric angular momentum and Earth-atmosphere exchange of angular momentum simulated in a general circulation model, *J. Geophys. Res.*, 102, 1931–1941.
- Murphy, J. (1988), The impact of ensemble forecasts on predictability, *Quart. J. Roy. Meteorol. Soc.*, 114, 463–493.
- Nastula, J., D. Salstein, and B. Kolaczek (2009), Patterns of atmospheric excitation functions of polar motion from high-resolution regional sectors, *J. Geophys. Res.*, 114,

B04,407.

Neale, R. B., C.-c. Chen, P. H. Lauritzen, D. L. Williamson, A. J. Conley, A. K. Smith, M. Mills, and H. Morrison (2010), Description of the NCAR community atmosphere model (CAM 5.0), *Tech. Rep. NCAR/TN-486+STR.*, National Center for Atmospheric Research.

Neef, L., S. Walther, K. Matthes, and K. Kodera (2014), Observations of stratospheric sudden warmings in Earth rotation variations, *J. Geophys. Res. Atmos.*, 119, 1–13, doi:10.1002/2014JD021621.

Neef, L. J., and K. Matthes (2012), Comparison of Earth rotation excitation in data-constrained and unconstrained atmosphere models, *J. Geophys. Res.*, 117(D2), D02,107, doi:10.1029/2011JD016555.

Paek, H., and H.-P. Huang (2012), A Comparison of Decadal-to-Interdecadal Variability and Trend in Reanalysis Datasets Using Atmospheric Angular Momentum, *J. Clim.*, 25(13), 4750–4758, doi:10.1175/JCLI-D-11-00358.1.

Pedatella, N. M., K. Raeder, J. L. Anderson, and H.-L. Liu (2013), Application of data assimilation in the Whole Atmosphere Community Climate Model to the study of day-to-day variability in the middle and upper atmosphere, *Geophys. Res. Lett.*, 40(16), 4469–4474, doi:10.1002/grl.50884.

Polavarapu, S., T. G. Shepherd, Y. Rochon, and S. Ren (2005), Some challenges of middle atmosphere data assimilation, *Quart. J. Roy. Meteorol. Soc.*, 131(613), 3513–3527, doi: 10.1256/qj.05.87.

Raeder, K., J. L. Anderson, N. Collins, T. J. Hoar, J. E. Kay, P. H. Lauritzen, and R. Pincus (2012), DART/CAM: An Ensemble Data Assimilation System for CESM

- Atmospheric Models, *J. Clim.*, 25(18), 6304–6317, doi:10.1175/JCLI-D-11-00395.1.
- Rosen, R. D., and D. A. Salstein (1985), Contribution of stratospheric winds to annual and semiannual fluctuations in atmospheric angular momentum and the length of day, *J. Geophys. Res.*, 90, 8033–8041.
- Rosen, R. D., and D. A. Salstein (2000), Multidecadal signals in the interannual variability of atmospheric angular momentum, *Clim. Dyn.*, 16, 693–700.
- Saha, S., et al. (2010), The NCEP Climate Forecast System Reanalysis, *Bull. Am. Meteorol. Soc.*, 91(8), 1015–1057, doi:10.1175/2010BAMS3001.1.
- Saynisch, J., and M. Thomas (2012), Ensemble Kalman-Filtering of Earth rotation observations with a global ocean model, *J. Geodyn.*, 62, 24–29, doi:10.1016/j.jog.2011.10.003.
- Saynisch, J., M. Wenzel, and J. Schröter (2010), Assimilation of Earth rotation parameters into a global ocean model: length of day excitation, *J. Geod.*, 85(2), 67–73, doi:10.1007/s00190-010-0416-0.
- Saynisch, J., M. Wenzel, and J. Schröter (2011), Assimilation of Earth rotation parameters into a global ocean model: excitation of polar motion, *Nonlinear Process. Geophys.*, 18(5), 581–585, doi:10.5194/npg-18-581-2011.
- Weickmann, K., S. Khalsa, and J. Escheid (1992), The atmospheric angular-momentum cycle during the tropical madden-julian oscillation, *Mon. Wea. Rev.*, 120, 2252–2263.
- Yamaguchi, M., S. T. K. Lang, M. Leutbecher, M. J. Rodwell, G. Radnoti, and N. Borman (2015), Observation-based evaluation of ensemble reliability, *Quart. J. Roy. Meteorol. Soc.*, doi:10.1002/qj.2675.
- Yu, N., D. Zheng, and H. Wu (1999), Contribution of new AAM data source to ΔLOD excitation, *J. Geod.*, 73, 385–390.

Zhou, Y., J. Chen, and D. Salstein (2008), Tropospheric and stratospheric wind contributions to earth's variable rotation from NCEP/NCAR reanalyses (2000-2005), *Geophys. J. Int.*, 174, 453–463, doi:10.1111/j.1365-246X.2008.03843.

Table 1. Overview of assimilation experiments performed.

Number	Model	Assimilated Quantities	Run dates
1	WACCM	none	1 Oct 2009 - 31 Mar 2010
2	WACCM	GPS-RO + NNRA ^a tropics only	1 Oct 2009 - 31 Mar 2010
3	WACCM	GPS-RO + NNRA ^a whole atmosphere	1 Oct 2009 - 31 Mar 2010
4	CAM	none	1 Jan - 28 Feb 2009
5	CAM	χ_1, χ_2, χ_3	1 Jan - 28 Feb 2009
6	CAM	Temperature	1 Jan - 31 Jan 2009
7	CAM	Temperature, χ_1, χ_2, χ_3	1 Jan - 17 Jan 2009

^a Observations used in the NCEP/NCAR Reanalysis project *Saha et al. [2010]*, which include radiosonde and aircraft winds and temperatures, plus satellite drift winds.

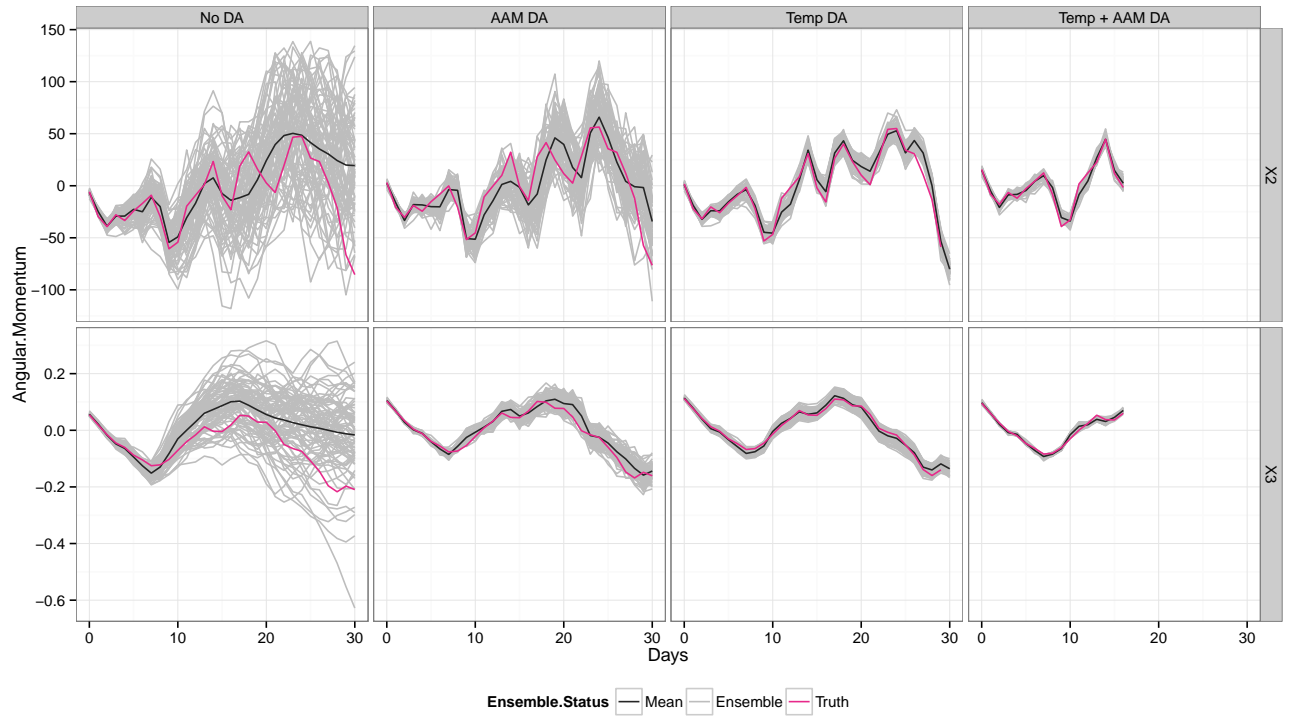


Figure 1. The DART-CAM prior ensemble (gray) and its mean (black) compared to the true state (pink) in terms of angular momentum components χ_2 and χ_3 , comparing four perfect-model experiments with DART-CAM (see text and Table 1).

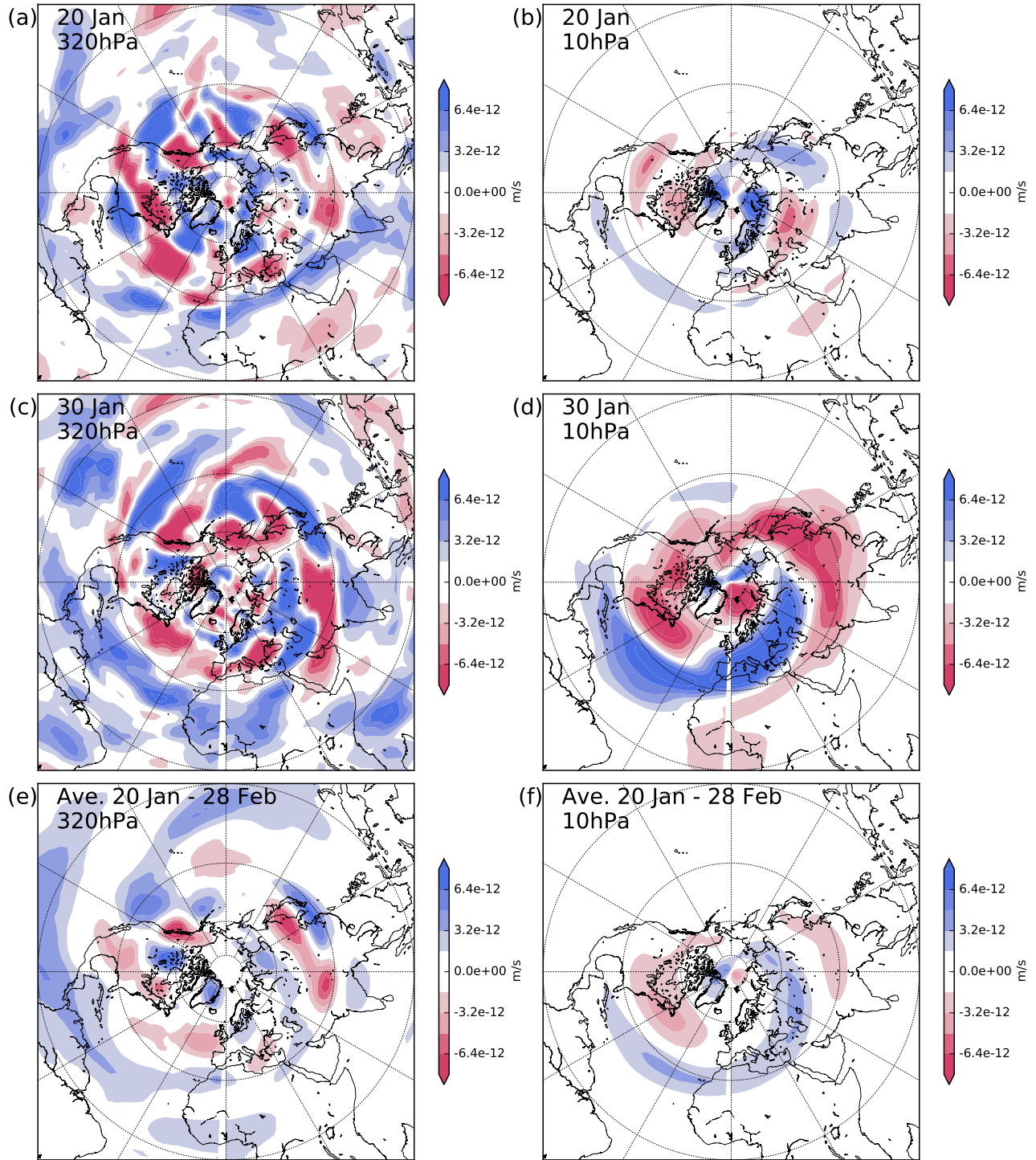


Figure 2. Snapshots of the covariance between the zonal wind and the axial angular momentum (χ_3) shortly after spin-up (top row), at the end of the assimilation period (middle row), and averaging over the entire period minus spinup time (bottom row), assimilating only the angular momentum. The lefthand column shows snapshots at 320 hPa; the righthand column shows snapshots at 10 hPa.

December 23, 2015, 1:17pm

D R A F T

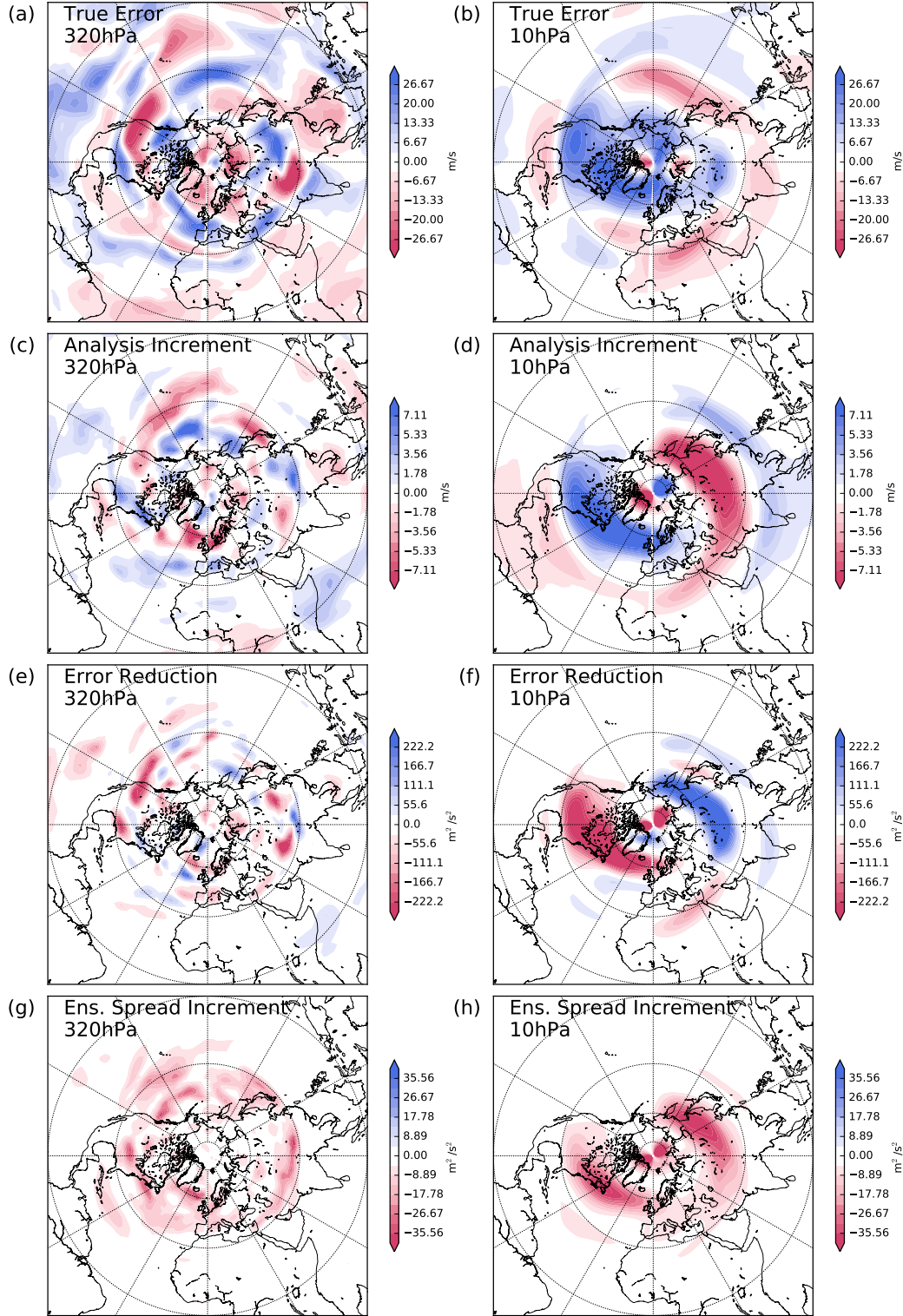


Figure 3. Snapshots of the 320 hPa zonal wind (a) true error (true minus prior ensemble mean), (b) analysis increment (posterior minus prior ensemble mean), (c) square error reduction (posterior minus prior mean square error), and (d) reduction in the ensemble spread (posterior minus prior, scaled as in (22)). All plots are shown for 30 Jan, for the CAM ensemble assimilating D R A F T December 23, 2015, 1:17pm D R A F T only atmospheric angular momentum.

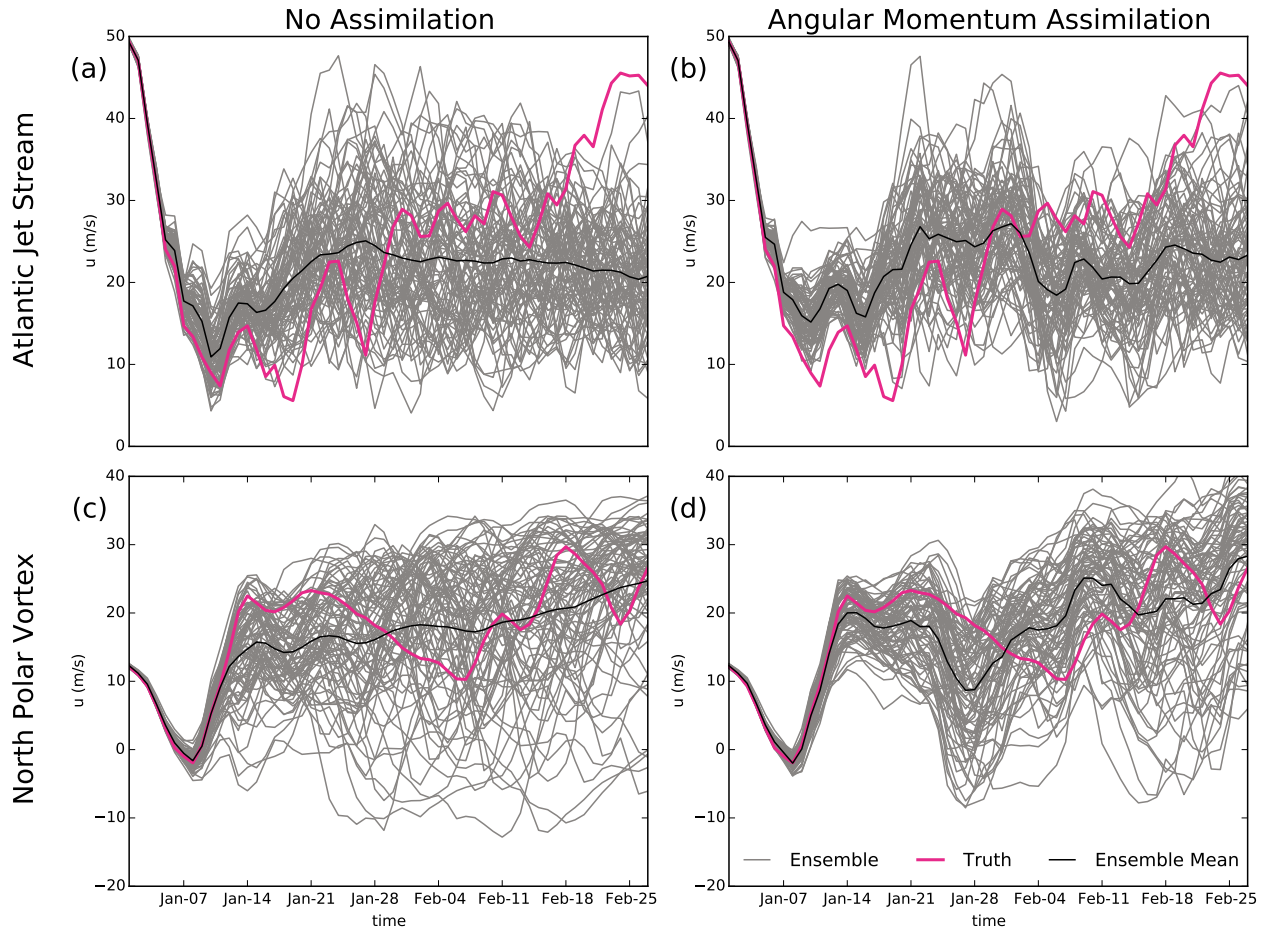


Figure 4. Comparison of the ensemble and its mean to the true state, comparing no assimilation (left column), and assimilation of the three angular momentum components (right column). The top row shows zonal wind averaged over the Atlantic jet stream, and the bottom row shows zonal wind averaged in the polar vortex (see text).

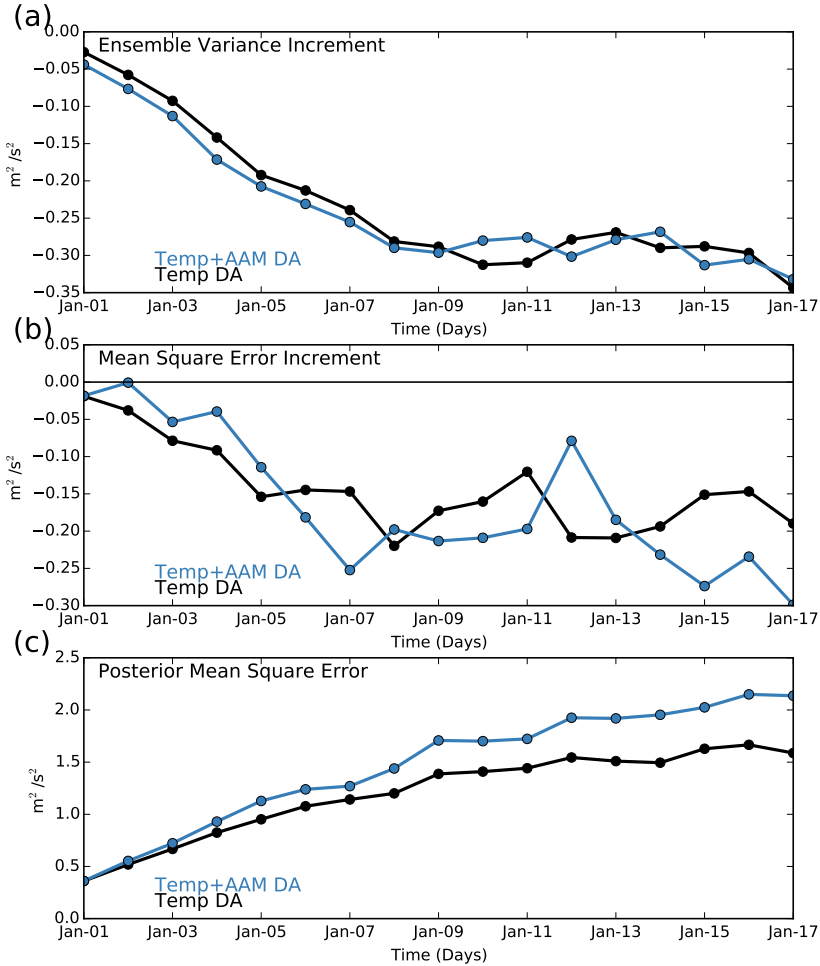


Figure 5. (a) Global average increment (posterior-prior) in the ensemble variance, scaled as in (22), for zonal wind in a DART-WACCM ensemble assimilating local temperatures (black) and temperatures along with atmospheric angular momentum (blue). (b) As in (a), but for the increment in the mean square error. (c) As above, but showing the absolute posterior mean square error.

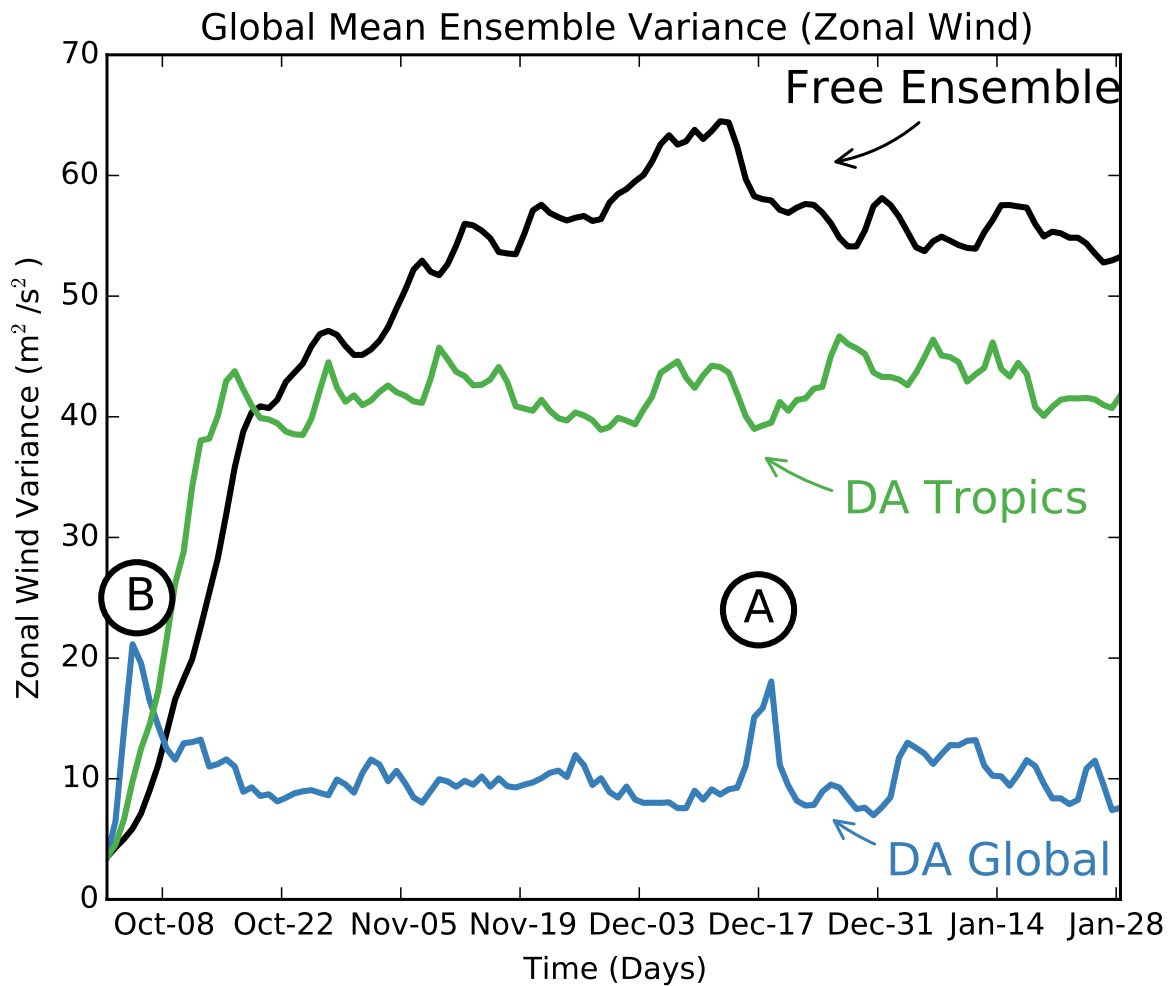


Figure 6. Global-average ensemble variance in the zonal wind as a function of time, comparing a DART-WACCM with no assimilation, and with 6-hourly assimilation of meteorological observations (see text).

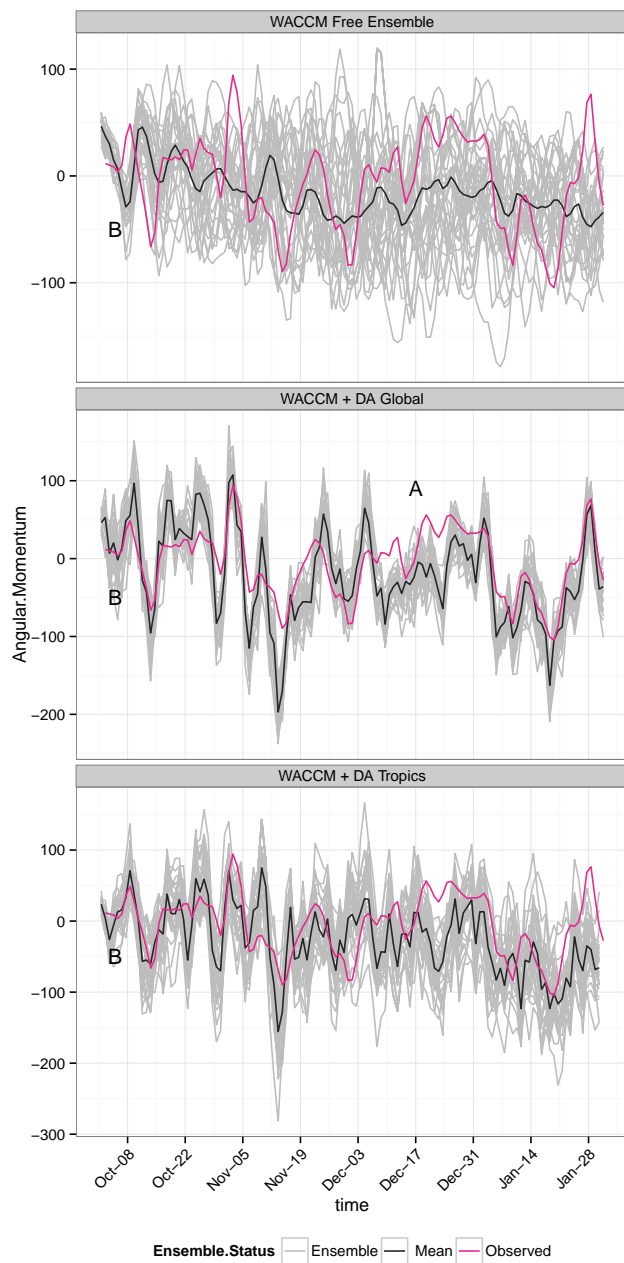


Figure 7. Comparison of the ensemble (gray) and its mean (black) in DART-WACCM experiments with increasing observational constraints (Table 1), in terms of angular momentum excitation functions χ_2 and χ_3 . Each angular momentum function is compared to the angular momentum implied by the corresponding Earth rotation parameters (pink).